BMJ Open Ophthalmology

Changes in the OCT angiographic appearance of type 1 and type 2 CNV in exudative AMD during anti-VEGF treatment

Henrik Faatz [1], Marie-Louise Farecki,[1] Kai Rothaus,[1] Matthias Gutfleisch,[1] Daniel Pauleikhoff,[1,2] Albrecht Lommatzsch[1,2,3]

Check for updates

¹Department of Ophthalmology, St. Franziskus Hospital Münster, Münster, Germany
²Department of Ophthalmology, University of Duisburg-Essen, Essen, Germany
³Achim Wessing Institute of Ophthalmic Diagnostic (AWIO), Essen, Germany

Correspondence to
Dr. Henrik Faatz; henrik.faatz@augen-franziskus.de

ABSTRACT

Objective Optical coherence tomography angiography (OCT-A) enables detailed visualisation of the vascular structure of choroidal neovascularisation (CNV). The aim of this study was to determine whether mathematically ascertained OCT-A vascular parameters of type 1 and type 2 CNV in exudative age-related macular degeneration (AMD) change during antivascular endothelial growth factor (anti-VEGF) treatment. The OCT-A vascular parameters were also compared with previously obtained activity parameters (fluid distribution on spectral domain OCT (SD-OCT)) to establish whether they could potentially be used as further 'activity parameters' for assessment of anti-VEGF treatment.

Methods and Analysis We evaluated 27 eyes of 27 patients (mean follow-up 9.8 months) with type 1, type 2 or mixed CNV who had received anti-VEGF treatment (IVAN scheme). The parameters analysed were area (aCNV), total length of all vessels (tlCNV), overall number of vascular segments (nsCNV) and fractal dimension (FD) of the CNV. The changes in each of these parameters were correlated with the central foveal thickness (CFT).

Results Regression and renewed perfusion of the CNV corresponded with the decrease or increase, respectively, of macular fluid distribution on SD-OCT. The increase and decrease of CFT during anti-VEGF treatment were highly significantly correlated with changes in FD (p<0.00001), aCNV (p<0.00001), tlCNV (p<0.00001) and nsCNV (p<0.00001).

Conclusion OCT-A enables detailed analysis of AMD with regard to FD, aCNV, tlCNV and nsCNV. As the changes in these parameters correlate closely with changes on SD-OCT, they can be used as new activity parameters, alongside fluid distribution, for assessment of treatment effect and as parameters of stabilisation or the need for repeated treatment.

Key messages

What is already known about this subject?
► Optical coherence tomography angiography (OCT-A) showed detailed visualisation of the vascular structure of choroidal neovascularisation (CNV).

What are the new findings?
► OCT-A enables detailed analysis of age-related macular degeneration with regard to fractal dimension, area, total length of all vessels and number of vascular segments of the CNV, and changes in these parameters correlate closely with changes on spectral domain OCT (SD-OCT).

How might these results change the focus of research or clinical practice?
► The new parameters could be used as new, additional activity parameters, alongside fluid distribution in SD-OCT.

INTRODUCTION

Technical advances in retinal imaging during recent decades have opened up new diagnostic options in retinology. The year 1961 saw the introduction of fluorescein angiography (FA), which detected retinal and choroidal vascular pathology by tracing the hyperfluorescent or hypofluorescent distribution of intravenously administered fluorescein.[1] Since 1973, indocyanine green (ICG) has also been used as a fluorescent dye for angiography in particular morphological circumstances. Because ICG binds almost completely to plasma proteins, it stays in the blood vessels for a longer time and shows less leakage. In 1991, optical coherence tomography (OCT) was introduced, initially permitting assessment of the retina and the vitreoretinal interface.[2] The development of spectral domain OCT (SD-OCT) yielded ever-improving resolution and shorter examination times, enabling differentiation of the individual layers—the inner and outer retinal layers, the retinal pigment epithelium (RPE), and the choroid—and established OCT as part of the retinal diagnostic work-up. The latest advance is OCT angiography (OCT-A), first described by Yu and Chen in 2010.[3] OCT-A yields new insights into the physiological and pathological blood flow in the retina and choroid, and is non-invasive in contrast to FA. The examination time is also shorter,

making OCT-A a much more patient-friendly procedure. The crucial difference compared with FA is the capacity for segmented visualisation of blood flow in all layers of the retina and choroid, adding new pathogenetic discussion points and concepts in combination with established imaging modalities. Multimodal imaging (SD-OCT, FA, ICG-A, OCT-A) is also helpful in the interpretation of pathogenetic relationships and monitoring during treatment of age-related macular degeneration (AMD). Timely diagnosis of exudative AMD (nAMD) and early detection of renewed activity during monitoring of anti-vascular endothelial growth factor (anti-VEGF) treatment administered as needed (pro re nata, PRN) are crucial for a good functional result.[4]

nAMD affects many layers of the inner and outer retina, the RPE, and the choroid. This necessitates a learning process with regard to interpretation of the blood flow findings in the individual segments particularly in the presence of pathological alterations in segmentation by any pigment epithelial detachments (PED). OCT-A permits representation of the morphological internal architecture of a choroidal neovascularisation (CNV) in relation to the perfused capillaries. These change under therapy and thus new biomarkers could emerge. In a previous study, we provided a mathematical description of the vascular parameters in type 1 and type 2 CNV and demonstrated significant changes in these parameters following initial anti-VEGF treatment (three injections).[5] We measured the area (aCNV), the total length of all vessels (tlCNV), the overall number of vascular segments (nsCNV) and the fractal dimension (FD) of the CNV.

The aim of this study was to analyse the changes in these mathematical parameters in patients requiring long-term anti-VEGF treatment and correlate them with the established SD-OCT parameters of activity.

PATIENTS AND METHODS

Twenty-seven eyes of 27 patients were included. A total of 115 visits were evaluated. In all patients the initial diagnosis of type 1, type 2 or mixed-type nAMD was determined by means of FA and SD-OCT (Spectralis HRA+OCT, Heidelberg Engineering, Heidelberg, Germany). In every case, history taking was followed by ophthalmic examination including best-corrected visual acuity, slit lamp microscopy and direct ophthalmoscopy using the slit lamp in mydriasis. In addition, OCT-A imaging (RTVue XR Avanti (Optovue, Fremont, California, USA) with AngioVue) was performed in all patients. The Avanti device generates 70 000 A-scans per second at a wavelength of 840 nm and has a penetration depth of 3 mm. The axial resolution is 5 µm, and the lateral resolution 22 µm. Images with dimensions of 3×3 mm and 6×6 mm were analysed. In each individual patient the same size of image was evaluated for all visits, with a preference for 3×3 mm. If the CNV extended beyond the edge of the image, 6×6 mm images were used. Patients with polypoidal choroidal vasculopathy or retinal angiomatous proliferations were excluded from the study. We also excluded those whose image quality was inferior (quality scores ≤5 and signal strength index ≤60). Patients with interruption in their attendance and therefore in imaging were excluded.

The patients were treated PRN with intravitreal anti-VEGF medications according to the prospective phase III IVAN (Inhibition of VEGF in Age-related Choroidal Neovascularisation) study,[6] and multimodal imaging was repeated after anti-VEGF treatment and in the event of new disease activity (figures 1 and 2). The criteria for activity were presence of subretinal fluid, persistence or increase of diffuse retinal thickening, increase in intraretinal cyst-like fluid spaces, and increased vascularised PED on SD-OCT.[7] The patients' mean follow-up was 9.8 months (SD 9.5 months). The central foveal thickness (CFT) was measured on SD-OCT images. For evaluation of the OCT-A images, we selected the 'outer retina' segment, which extends from 9 µm under the outer plexiform layer to 9 µm above the Bruch's membrane. In order to achieve more accurate and complete documentation of type 1 CNV, this segment was manually displaced by 18 µm towards the choroid. The automatic 'remove artifact' function was used to minimise artefacts. First the physician exports the en-face OCT-A images from the ReVue software and saves them loss-less as TIFF files. These images are imported to Fiji (National Institute of Mental Health, Bethesda, Maryland, USA), where the CNV is interactively segmented into a polygon. Everything except the CNV is then removed so that the subsequent automated Matlab program (V.R2014b, MathWorks) is able to analyse the CNV morphology. The
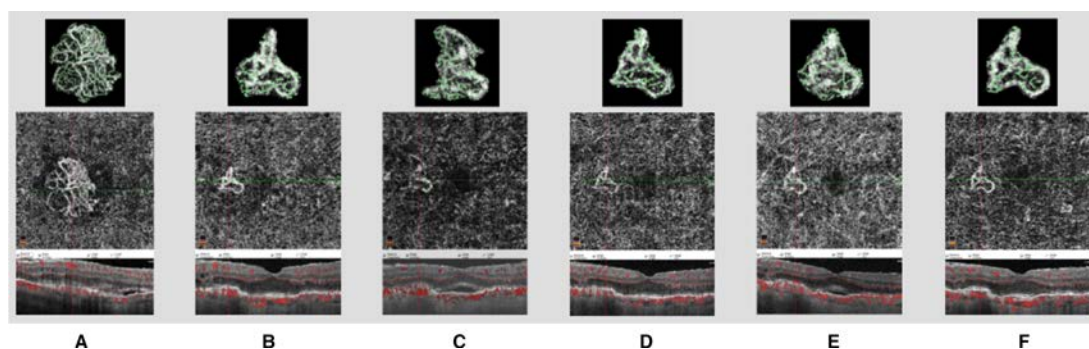

Figure 1 Type 2 CNV on OCT-A with the corresponding B-scans and vascular diagrams at initial diagnosis (a), after anti-VEGF treatment in the inactive phase (b) and later with renewed activity (c, e) and inactivity following anti-VEGF treatment (d, f).
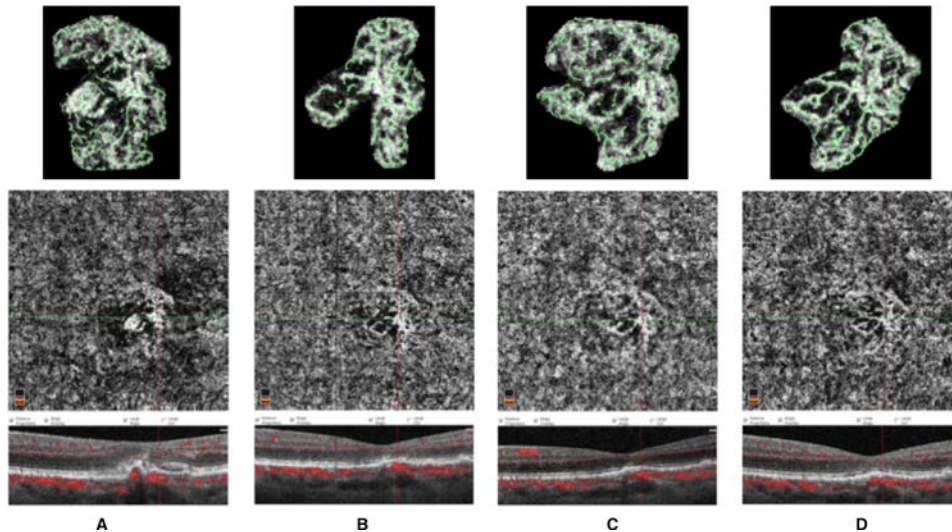
Figure 2 Type 1 CNV on OCT-A with corresponding B-scans and vascular diagrams at initial diagnosis (a), after anti-VEGF treatment in the inactive phase (b, d) and with renewed activity (c).

gradient field is computed using the Nabla operator. We achieved this by weak Gaussian smoothing followed by one-pixel finite difference of the image in the x and y directions. The edge strength is then enhanced and multiscale smoothing is performed to propagate the edge information towards the skeleton lines.[8] For detection of the ridges, which correspond to the vasculature, again the Nabla operator is applied to the smoothed gradient field. Technically, this approach corresponds to multiscale application of the Laplace operator and the result can be interpreted as creaseness of the image.[9] Exclusion of all pixels with less than maximal creaseness leaves the skeleton pixels of the vasculature. Finally, the skeleton pixels are grouped to form smooth vessel segments connected by nodes at bifurcations or crossings. Based on the CNV skeleton and the vascular graph, we computed the aCNV, FD, tlCNV and nsCNV.[10]

Statistical analyses were performed using R V.x64, 3.2.5. First the Shapiro-Wilk test was used to determine whether the parameters of interest were normally distributed, then a paired t-test was carried out because the sample size was over 50. A Spearman correlation test was performed to calculate the correlations. The level of significance for all tests was 5%.

Patient and public involvement statement

All attendees brought patient information. Data acquisition was retrospective. There was no additional effort for the patients.

RESULTS

With regard to function, a positive correlation was observed between vision and CFT (p=0.00002, r=0.391). The mean CFT of all study participants at baseline was 327.45 μm (median 316 μm; SD ±64.1 μm). As expected, there was a significant difference in mean CFT between the inactive and the active phase of CNV (288.5 μm vs 356.3 μm; p<0.00001).

The mean aCNV in en-face view was 1.34 mm² (median 0.79 mm²; SD ±1.52 mm²). Dividing the patients according to the presence or absence of CNV activity on SD-OCT, we found a significant mean difference (p=0.007) between patients in the inactive phase (0.9 mm²) and those in the active phase (1.7 mm²) of disease (figure 3A). Correlation of the results in two successive examinations, that is, the change from one examination to the next in each individual patient, showed a positive, highly significant association between aCNV and CFT (p<0.00001, r=0.690) (figure 4A).

The mean tlCNV was 9.48 mm (median 5.44 mm; SD ±9.56 mm). Dividing the patients according to the presence or absence of CNV activity on SD-OCT, we found a significant mean difference (p=0.003) between patients in the inactive phase (6.6 mm²) and those in the active phase (11.6 mm²) of disease (figure 3B). Correlation of the results in two successive examinations, that is, the change from one examination to the next in each individual patient, showed a positive, highly significant association between tlCNV and CFT (p<0.00001, r=0.682) (figure 4B).

The mean nsCNV was 122.9 (median 79.0; SD ±122.6). Dividing the patients according to the presence or absence of CNV activity on SD-OCT, we found a significant mean difference (p=0.003) between patients in the inactive phase (82.8) and those in the active phase (152.6) of disease (figure 3C). Correlation of the results in two successive examinations, that is, the change from one examination to the next in each individual patient, showed a positive, highly significant association between nsCNV and CFT (p<0.00001, r=0.671) (figure 4C).

The mean FD of the CNV was 1.20 (median 1.22; SD ±0.17). Dividing the patients according to the presence or absence of CNV activity on SD-OCT, we found a significant mean difference (p=0.003) between patients in the inactive phase (1.15) and those in the active phase (1.25) of disease (figure 3D). Correlation of the results
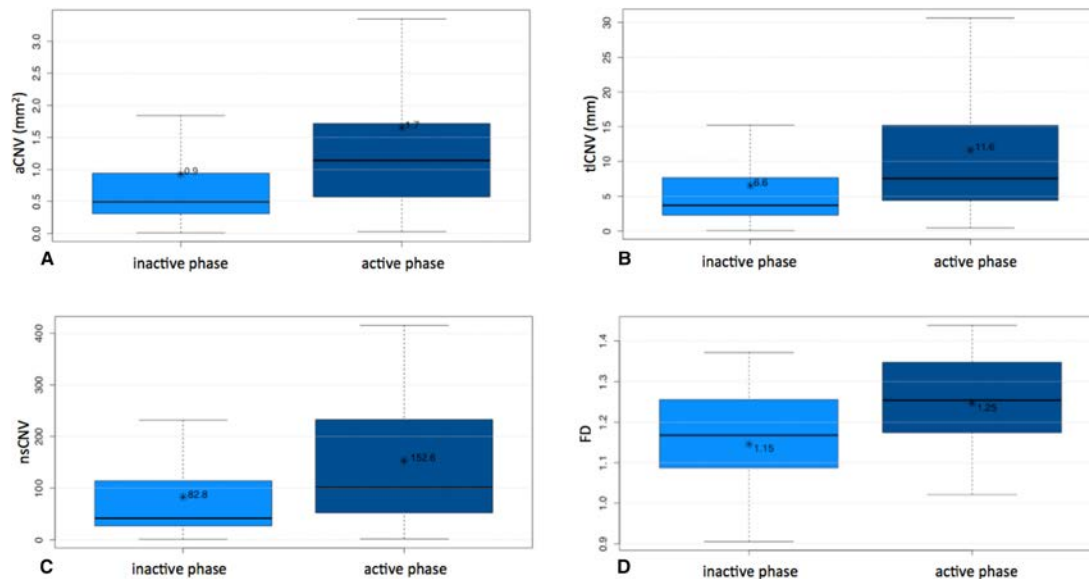
Figure 3 aCNV, area of CNV; CNV, choroidal neovascularisation; FD, fractal dimension; nsCNV, number of vascular segments; tlCNV, total length of all vessels, * mean value. Comparison of (a) aCNV (mm²) in the active and inactive phase; (b) tlCNV (mm) in the active and inactive phase; (c) nsCNV in the active and inactive phase; (d) FD in the active and inactive phase.

in two successive examinations, that is, the change from one examination to the next in each individual patient, showed a positive, highly significant association between nsCNV and CFT (p<0.00001, r=0.626) (figure 4D).

DISCUSSION

OCT-A performs very well in detecting type 1 and type 2 CNV, with sensitivity of 86% and specificity of 82 %.[11] The central question is primarily whether OCT-A can replace FA or whether OCT-A can be viewed as a complementary imaging modality, with the two procedures together yielding much greater sensitivity than either method

alone.[12] If further evaluations of OCT-A were to underscore the validity of its characterisation of treatment-relevant CNV morphology, then OCT-A could be used alone for confident diagnosis in the future—certainly a desirable scenario. However, even now CNV can be analysed not only in the active stage, but also in the inactive stage following anti-VEGF treatment.[5 13 14] OCT-A also detects 'silent' CNV that has led to neither intraretinal nor subretinal fluid and cannot be depicted on SD-OCT or FA.[15 16] To the present time, however, there is no clear criteria for CNV activity on OCT-A, so no conclusions can be drawn whether a detected CNV is active or inactive.
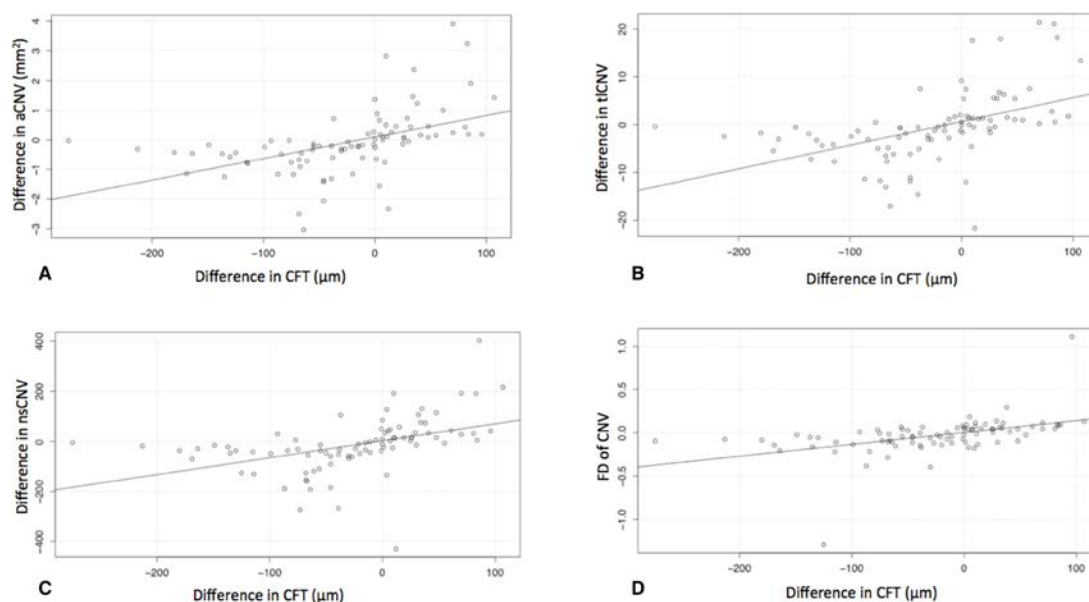

Figure 4 aCNV, area of CNV; CFT, central foveal thickness; CNV, choroidal neovascularisation; FD, fractal dimension; nsCNV, number of vascular segments; tlCNV, total length of all vessels. Significant correlation between (a) difference in aCNV (mm²) and difference in CFT (µm); (b) difference in tlCNV (mm) and difference in CFT (µm); (c) difference in nsCNV and difference in CFT (µm); (d) difference in FD of CNV and differende in CFT (µm).

In CNV, pathological vessels grow from the choriocapillaris into the retina. These vessels indicate permeability disorders by leaking fluid at subpigment epithelial, subretinal and/or intraretinal locations. SD-OCT is therefore used to monitor the results of treatment. The presence of subretinal fluid or an increase in subpigment epithelial or intraretinal fluid constitutes a criterion of activity and thus indicates renewed treatment in the IVAN PRN scheme (three injections at 4-week intervals). Thus, with this means of assessment, one can conclude only indirectly that changes in the CNV have taken place.

Lumbroso et al[17] observed the vascular morphology of CNV and sought to arrive at conclusions regarding the treatment required. Huang et al[18] also described distinct regression of CNV visualised by differences in blood flow in the first 2 weeks after anti-VEGF treatment, with a renewed increase in visualisable CNV after 4 weeks and then an increase in fluid collections. Muakkassa et al[19] showed regression of CNV area following anti-VEGF treatment with associated regression of subretinal and/or intraretinal fluid.

We have already shown in a previous study that the mathematical analyses of 'skeletonized' vessels also used in this study are able to quantify the progressive vascular changes in macular telangiectasia type 2.[10] This procedure was again used in the present study and showed that the various mathematical characteristics of the vessels may be significantly correlated with the established alterations (fluid distribution on SD-OCT) between inactive and active disease. Previous publications described the morphological patterns of neovascular membranes such as a medusa or sea-fan-shaped pattern or an ill-defined pattern without any correlation with clinical activity.[20–22] More specific data on these vascular changes during treatment might therefore identify new parameters for assessment of CNV activity. This could lead to early diagnosis when activity increased and thus to faster initiation of treatment, which is crucial to the patient's visual outcome.[4] aCNV can be documented very accurately by OCT-A. It is extremely important CNV is captured completely in the selected segment, or the CNV will appear smaller than its true size. Previous publications have shown a significantly smaller aCNV on OCT-A than on FA and ICG-A.[23–25] One possible reason for this is that the leakage effect caused by FA and ICG-A due to the abnormal permeability of the vessels magnifies the apparent extent of the CNV. The correlation between the increase and decrease of aCNV and the increase and decrease of CFT, together with the significantly smaller area in the inactive phase of disease, shows that OCT-A achieves more precise analysis of the area and therefore more accurate detection of activity changes at the level of the vessels themselves. Other authors have also described a significant decrease in aCNV after anti-VEGF treatment and a renewed increase possibly accompanied by exudation.[13 26] In contrast, Xu et al[27] described a general increase in the size of CNV under anti-VEGF therapy, and Carnevali et al[28] observed a growth in size

of quiescent CNV without correlation to clinical activity. Bailey et al[29] found, in eyes with non-exudative CNV, a CNV area growth rate of 20% per month associated with a high risk to develop exudation. Therefore size change of aCNV could be one important parameter for assessment of CNV activity. It should be noted that OCT-A only represents perfusion in a defined observation window and changes are thus related to the fact that vascular parts are no longer perfused or are perfused more slowly. During reactivation, however, these were again visible as perfused. Therefore the change of the CNV size can only be interpreted as an increase or decrease of the perfused CNV area and not of the real vessel size.

Earlier studies showed that the capillaries visible in a CNV decrease during anti-VEGF treatment, whereas the prominent afferent vessels change little or not at all.[30] This is interpreted as a consequence of heightened sensitivity of the capillaries compared with mature vessels owing to the lack of pericytes, which makes them vulnerable to anti-VEGF. The results of our study show that, in the mathematical model we used, tlCNV decreased significantly on treatment. Depletion of anti-VEGF is often followed by renewed disease activity with exudation and increasing CFT. This is in accordance with our finding that tlCNV also increases and correlates with the change in CFT during the course of treatment. Further research is required, however, to determine the extent to which these mathematical parameters can map the 'maturation' of CNV to primarily larger mature vessels. Given that nsCNV decreased significantly with longer-term treatment in our study, this application of the CNV quantification method we used seems to have realistic potential. This is in agreement with the above-mentioned findings of earlier studies where the small segments of CNV vessels disappeared during treatment but the prominent segments were preserved.[30] The mathematical model could thus enable objective analysis of vascular changes in CNV that reflect direct biological effects on the CNV and may therefore represent an additional means of assessing the effects of treatment over time. This is backed up by the significant correlation we observed between changes in nsCNV and changes in CFT.

We used FD as a parameter to represent objectively the complexity of the vascular structure of CNV. FD was significantly lower in the inactive phase of CNV than in the active phase. This shows that the vascular structure becomes less complex, that is, the numbers of vascular segments and branches decrease. As mentioned above, studies have already shown that anti-VEGF treatment particularly reduces the small-calibre CNV vessels, while the large-calibre vessels remain unaffected.[17 18 30 31] To date, however, these assessments of treatment effects have always been subjective; there has been no objective means of quantifying the changes. This gap is filled by FD. Al-Sheikh et al[32] also compared the FD of active and inactive CNV in nAMD and found a significantly lower value in the inactive phase, in accordance with our findings. The significant correlation between the change in

FD and the change in CFT shows agreement with previously used parameters of activity.

The limitations of our study include the small study population and that the CNV had to be marked manually. This is heavily dependent on the investigator's experience with OCT-A and on the resolution, which is limited by the manufacturer's technical specifications. The agreement among expert assessors of OCT-A findings in CNV is comparable with that for FA.[33] Second, the image quality is crucial for all subsequent mathematical analyses of OCT-A images. The quality has already been greatly improved by the development of eye-tracking systems to avoid movement artefacts. Projection artefacts also limit the accuracy of detection of CNV and their quantification. Moreover, the segmentation in any given patient can change in the course of time, because the morphology of the retina is usually markedly changed by the withdrawal of intraretinal and/or subretinal fluid, with the result that the segmentation levels generated by the manufacturer may also change. Furthermore, the information yielded by OCT-A is limited by the fact that the data are two-dimensional. The future goal should be to depict CNV in three dimensions on OCT-A in order to permit comprehensive assessment and to validate the observed associations in large, reading centre-based studies.

ORCID iD
Henrik Faatz http://orcid.org/0000-0002-5363-0052

REFERENCES
1 Novotny HR, Alvis DL. A method of photographing fluorescence in circulating blood in the human retina. *Circulation* 1961;24:82–6.
2 Huang D, Swanson EA, Lin CP, *et al*. Optical coherence tomography. *Science* 1991;254:1178–81.
3 Yu L, Chen Z. Doppler variance imaging for three-dimensional retina and choroid angiography. *J Biomed Opt* 2010;15:016029.
4 Matthé E, Sandner D. Frühzeitige Behandlung MIT ranibizumab (Lucentis®) bei exsudativer AMD. *Ophthalmologe* 2011;108:237–43.
5 Faatz H, Farecki M-L, Rothaus K, *et al*. Optical coherence tomography angiography of types 1 and 2 choroidal neovascularisation in age-related macular degeneration during anti-VEGF therapy: evaluation of a new quantitative method. *Eye* 2019;33:1466–71.
6 Wintergerst MWM, Larsen PP, Heimes B, *et al*. [Pro re nata anti-VEGF treatment results for neovascular age-related macular degeneration in routine clinical treatment: comparison of single with triple injections]. *Ophthalmologe* 2019;116.
7 Deutsche Ophthalmologische Gesellschaft. [Anti-VEGF therapy for neovascular age-related macular degeneration -therapeutic strategies: statement of the German Ophthalmological Society, the German Retina Society and the Professional Association of Ophthalmologists in Germany - November 2014]. *Ophthalmologe* 2015;112:237–45.
8 Rothaus K, Jiang X. Multi-scale Midline Extraction Using Creaseness. In: *Pattern recognition and image analysis*. Springer, Berlin, Heidelberg, 2005: 502–11.
9 López AM, Lloret D, Serrat J, *et al*. Multilocal Creaseness based on the Level-Set extrinsic curvature. *Comput Vis Image Und* 2000;77:111–44.
10 Pauleikhoff D, Gunnemann F, Book M, *et al*. Progression of vascular changes in macular telangiectasia type 2: comparison between SD-OCT and OCT angiography. *Graefes Arch Clin Exp Ophthalmol* 2019;257:1381–92.
11 Souedan V, Souied EH, Caillaux V, *et al*. Sensitivity and specificity of optical coherence tomography angiography (OCT-A) for detection of choroidal neovascularization in real-life practice and varying retinal expertise level. *Int Ophthalmol* 2018;38:1051–60.
12 Inoue M, Jung JJ, Balaratnasingam C, *et al*. A comparison between optical coherence tomography angiography and fluorescein angiography for the imaging of type 1 neovascularization. *Invest Ophthalmol Vis Sci* 2016;57.
13 McClintic SM, Gao S, Wang J, *et al*. Quantitative evaluation of choroidal neovascularization under pro re NatA anti-vascular endothelial growth factor therapy with OCT angiography. *Ophthalmol Retina* 2018;2:931–41.
14 Pilotto E, Frizziero L, Daniele AR, *et al*. Early OCT angiography changes of type 1 CNV in exudative AMD treated with anti-VEGF. *Br J Ophthalmol* 2019;103:67–71.
15 Palejwala NV, Jia Y, Gao SS, *et al*. Detection of NONEXUDATIVE choroidal neovascularization in age-related macular degeneration with optical coherence tomography angiography. *Retina* 2015;35:2204–11.
16 Roisman L, Zhang Q, Wang RK, *et al*. Optical coherence tomography angiography of asymptomatic neovascularization in intermediate age-related macular degeneration. *Ophthalmology* 2016;123:1309–19.
17 Lumbroso B, Rispoli M, Savastano MC. Longitudinal optical coherence tomography-angiography study of type 2 naive choroidal neovascularization early response after treatment. *Retina* 2015;35:2242–51.
18 Huang D, Jia Y, Rispoli M, *et al*. Optical coherence tomography angiography of time course of choroidal neovascularization in response to anti-angiogenic treatment. *Retina* 2015;35:2260–4.
19 Muakkassa NW, Chin AT, de Carlo T, *et al*. Characterizing the effect of anti-vascular endothelial growth factor therapy on treatment-naive choroidal neovascularization using optical coherence tomography angiography. *Retina* 2015;35:2252–9.
20 Karacorlu M, Sayman Muslubas I, Arf S, *et al*. Membrane patterns in eyes with choroidal neovascularization on optical coherence tomography angiography. *Eye* 2019;33:1280–9.
21 Souied EH, El Ameen A, Semoun O, *et al*. Optical coherence tomography angiography of type 2 neovascularization in age-related macular degeneration. *Dev Ophthalmol* 2016;56:52–6.
22 Kuehlewein L, Bansal M, Lenis TL, *et al*. Optical coherence tomography angiography of type 1 neovascularization in age-related macular degeneration. *Am J Ophthalmol* 2015;160:739–48.
23 Costanzo E, Miere A, Querques G, *et al*. Type 1 choroidal neovascularization lesion size: indocyanine green angiography versus optical coherence tomography angiography. *Invest Ophthalmol Vis Sci* 2016;57.
24 Takayama K, Ito Y, Kaneko H, *et al*. Comparison of indocyanine green angiography and optical coherence tomographic angiography in polypoidal choroidal vasculopathy. *Eye* 2017;31:45–52.
25 Told R, Sacu S, Hecht A, *et al*. Comparison of SD-Optical coherence tomography angiography and indocyanine green angiography in type 1 and 2 neovascular age-related macular degeneration. *Invest Ophthalmol Vis Sci* 2018;59:2393–400.
26 Torrecillas-Picazo R, Cerdà-Ibáñez M, Almor Palacios I, *et al*. Analysis and follow-up of type 1 choroidal neovascularisation with optical coherence tomography-angiography after antiangiogenic treatment. *Arch Soc Esp Oftalmol* 2017;92:265–72.
27 Xu D, Dávila JP, Rahimi M, *et al*. Long-Term progression of type 1 neovascularization in age-related macular degeneration using optical coherence tomography angiography. *Am J Ophthalmol* 2018;187:10–20.
28 Carnevali A, Sacconi R, Querques L, *et al*. Natural history of treatment-naïve quiescent choroidal neovascularization in age-

related macular degeneration using OCT angiography. *Ophthalmol Retina* 2018;2:922–30.

29 Bailey ST, Thaware O, Wang J, *et al*. Detection of Nonexudative choroidal neovascularization and progression to exudative choroidal neovascularization using OCT angiography. *Ophthalmol Retina* 2019;3:629–36.

30 Spaide RF. Optical coherence tomography angiography signs of vascular Abnormalization with antiangiogenic therapy for choroidal neovascularization. *Am J Ophthalmol* 2015;160:6–16.

31 Kuehlewein L, Dansingani KK, de Carlo TE, *et al*. Optical coherence tomography angiography of type 3 neovascularization secondary to age-related macular degeneration. *Retina* 2015;35:2229–35.

32 Al-Sheikh M, Iafe NA, Phasukkijwatana N, *et al*. Biomarkers of neovascular activity in age-related macular degeneration using optical coherence tomography angiography. *Retina* 2018;38:220–30.

33 Lindner M, Fang PP, Steinberg JS, *et al*. Oct Angiography-Based detection and quantification of the neovascular network in exudative AMD. *Invest Ophthalmol Vis Sci* 2016;57:6342–8.